Numerical Investigations on High Lift Force Generation of 3D Dragonfly Wing during Hovering Motions

Numerical Investigations on High Lift Force Generation of 3D Dragonfly Wing during Hovering Motions

Xiaohui Su[1], Kaixuan Zhang[1], Juan Zheng[1], Jiantao Zhang[1], Yong Zhao[2]

[1.]School of Hydraulic Engineering, Dalian University of Technology, Dalian 116024, China
[2.]College of Engineering, Nazarbayev University, 53 Kabanbaybatyr Ave., Astana, 010000, Republic of Kazakhstan

[*]Corresponding author e-mail: zkx@mail.dlut.edu.cn

Abstract. In the paper, a novel numerical method is present to numerically investigate life force generation mechanisms of 3D dragonfly wing during hovering motions. The dynamic mesh which descripts the motion of 3D wing and gird change in inner computational domain is generated by an ALE model we developed. Then the mesh is transferred at each time step into ANSYS CFX using Junction Box Routine. The simulation results show that a high lift force generated by implementing one specified advanced flapping action during hovering motion in which the translation time period of downstroke is shortened.

1. Introduction

The dragonfly flight mode existing in nature has long been the inspiration source for human beings to design Micro Air Vehicles (MAVs) which would be widely used in the field of national defense and civil field. Great progress literature reviews [1-4] summarized the aerodynamics of insect flight and the lift generation mechanism of rigid wing.

In this paper, the aerodynamic performance and energy consumption of dragonfly's wings during hovering flight are simulated with the geometrical model used in reference [5] which is simplified based on a real geometric parameters of Aeschna juncea hindwings [6,7] in 1972.

Moreover, a new rotation mode only by changing the beginning time of the down stroke reversal is present and the aerodynamic performance of the new rotation motion is numerically investigated.

2. Geometry of Hindwing and Kinematics

2.1 Geometry of dragonfly hindwing

The hindwing model is described as a rigid plate with a span length of R, 4.6 *cm*, average chord length of c, 1.12 *cm*, and a thickness of 1% of average chord length, about 0.0112 *cm*. The symmetric plane is located at 0.61 *cm* away from the wing root, and the rotation axis of the Angle of Attack (AOA) is 0.28 *cm* away from the leading edge c/4. The simplified geometric model of the dragonfly's hindwing is plot in Figure 1.

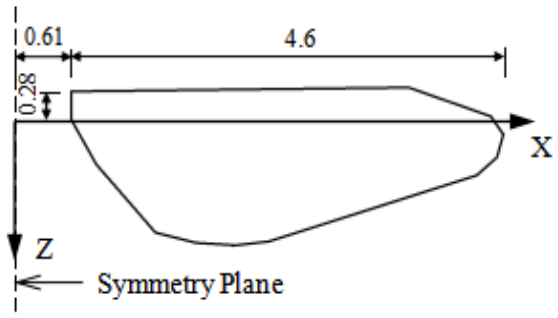

Figure 1. Simplified geometric model of the dragonfly hindwing

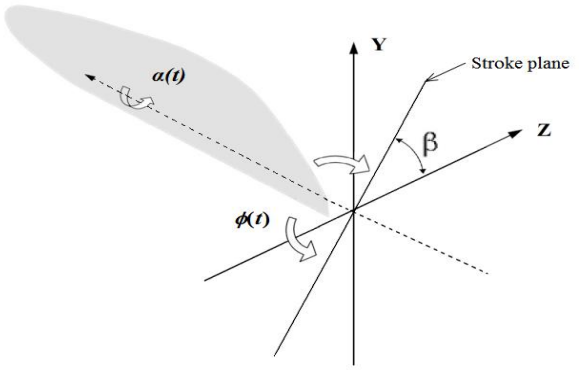

Figure 2. The sketch of the flapping motion of wing

2.2 The traditional kinematics of flapping motion

The flapping function of dragonfly wing during hovering flight is the same as the formula used in reference [5], as shown in Figure 2. It assumes that flapping plane and horizontal plane have an inclined angle β, 52°, deviation angle, 0°. Thus, only two parameters, flapping angle and AOA, control the movement of dragonfly wing. Flapping frequency is set to 36 *Hz*.

The flapping angle, $\Phi(t)$ and AOA, $\alpha(t)$ are described in Eqs. (1) and (2).

$$\varphi(t) = \varphi_0[\cos(2\pi ft) - 1] \tag{1}$$

where $\varphi_0 = 0.602$.

During the reversal of the stroke, the change of the angle of attack with time is described as follows:

$$\alpha(t) = 0.5\dot{\alpha}_0 \left[(t - t_r) - \frac{\Delta t_r}{2\pi} \sin(2\pi \frac{t - t_r}{\Delta t_r}) + \frac{\Delta t_r}{2} \right] \quad t_r \le t \le t_r + \Delta t_r \tag{2}$$

where, $\dot{\alpha}_0$ =20000 degree/s, Δt_r is the duration of wing flip and t_r is the time of wing flip.

The profiles of flapping angle, angle of attack and their respective angular velocity in one cycle are shown in Figure 3.

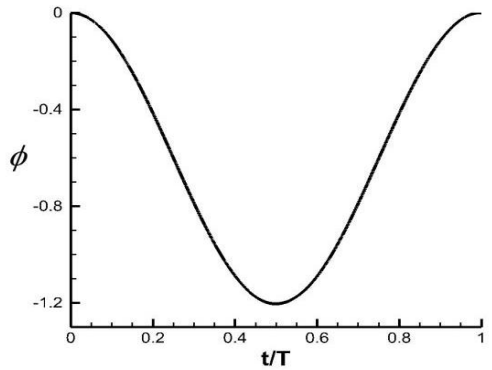

(a) Flapping angle

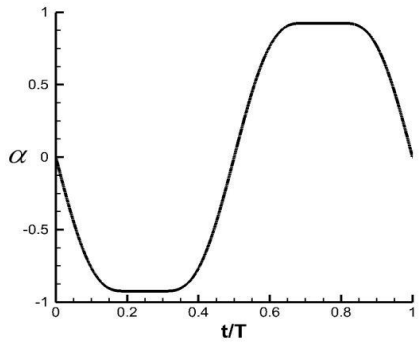

(b) Attack angle

Figure 3. The flapping angle and attack angle in one period

2.3 The model setup

The ANSYS CFX is used to solve the NS equations. In the model, air density $\rho = 1.185\ kg/m^3$ and

dynamic viscosity $\mu = 1.831 \times 10^{-5}\ kg \cdot m^{-1} \cdot s^{-1}$ are set in a still air. Transient analysis calculates 30 cycles to ensure the final solution in one period to attain convergence status. Time step is set to $5.56 \times 10^{-6}\ s$. The far field and moving boundary conditions are selected opening and non-slip wall boundary condition respectively.

2.4 Mesh convergence test

There are four meshes used to verify the convergence. The total mesh cells of the model are: 35566, 68497, 113614 and 233150 which can be found in Table 1.

Table 1. Mesh information

Mesh model	Wing surface mesh	Total mesh	Node point
Mesh1	1,024	35,566	6,566
Mesh2	1,024	68,497	12,058
Mesh3	2,786	113,614	19,995
Mesh4	6,084	233,150	40,746

Four monitoring points were picked up along the edge of the wing model shown in Figure 4. The instantaneous pressure values of those monitoring points are shown in Figure 5.

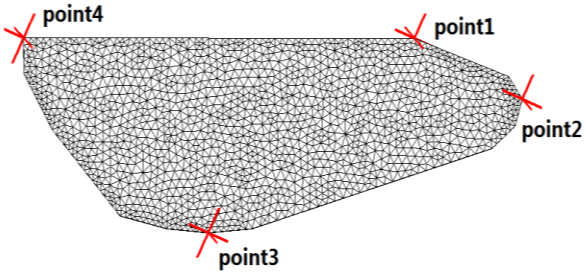

Figure 4. The position of the monitoring points on the wing model

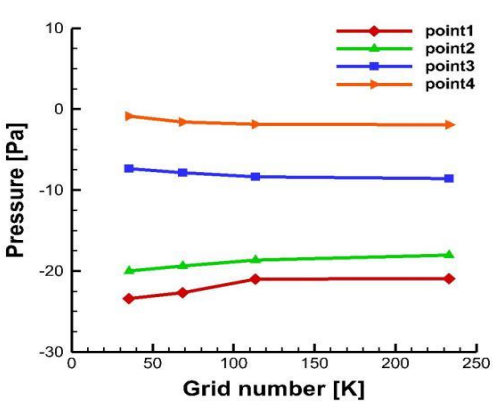

Figure 5. The instantaneous pressure values of the monitoring points under different grids

Figure 5 shows that with the increasing of mesh number, the instantaneous pressure values of the four monitoring points gradually trend to stable values. When the mesh amount increases to the third and the fourth series of meshes, the relative error of the instantaneous pressure values is below 3.24%. Therefore, the mesh could be considered reaching the convergence. Taking into account for the requirements of computational accuracy and time cost, the third set of grids is used as the computational mesh for subsequent studies.

2.5 Aerodynamic performance

In the study of insect flapping flight, the lift force coefficient, Cl and thrust coefficient, CT are most important to characterize the aerodynamic force. In the paper, the Cl denotes the aerodynamic component perpendicular to horizontal plane pointing to Y-Axis for lifting the weight of dragonfly while the CT represents the aerodynamic component orthogonal to the Cl direct to the Z-Axis. The Cl and CT are obtained by Eqs. (3) and (4) as followed.

$$CL = \frac{F_Y}{0.5\rho U^2 S_h} \tag{3}$$

$$CT = \frac{F_Z}{0.5\rho U^2 S_h} \tag{4}$$

where, $U = 4.0724$ *m/s*, is the dimensionless speed. S_h is the hindwing area, 5.152 cm^2.

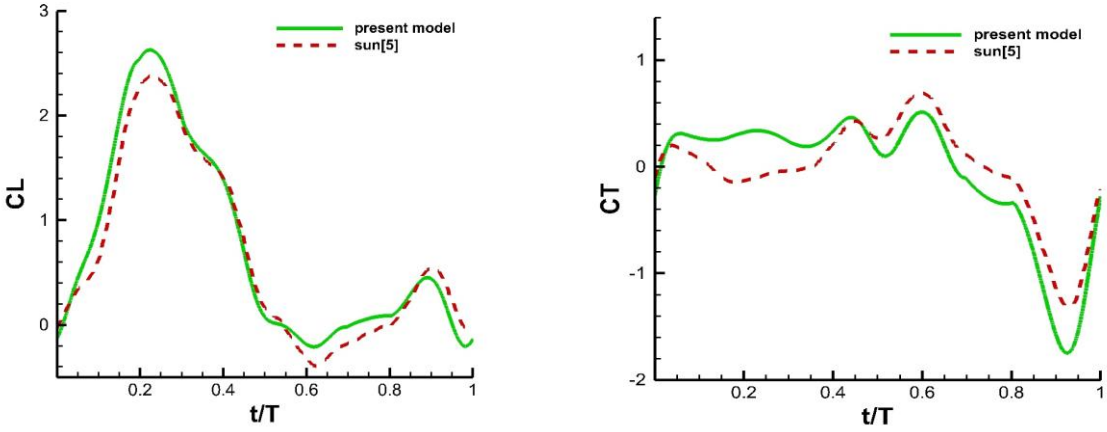

Figure 6. The profiles of CL and CT in one hovering motion cycle.

The Cl and CT are plot in Figure 6 and the results obtained by [5] are also plot for the comparison purpose. Figure 2.6 shows that the simulation results of the present model are approximately agreement with those in [5]. The period-averaged Cl of the present model during one period is 0.736 while the period-averaged Cl of reference [5] is 0.675. The relative error is about 9%.

3. The novel advanced model

In the paper, we present a novel advanced model in which the action of rapid pitch starts advanced before the traditional time moment, meaning the translation time of wing in downstroke becomes shorten and the translation time in upstroke becomes longer (seen in Figure 7). The advanced times in one flapping period, such as 2%, 4%, 6% and 8%, by comparing with the symmetry model, explored the effects on the aerodynamic characteristics of dragonfly.

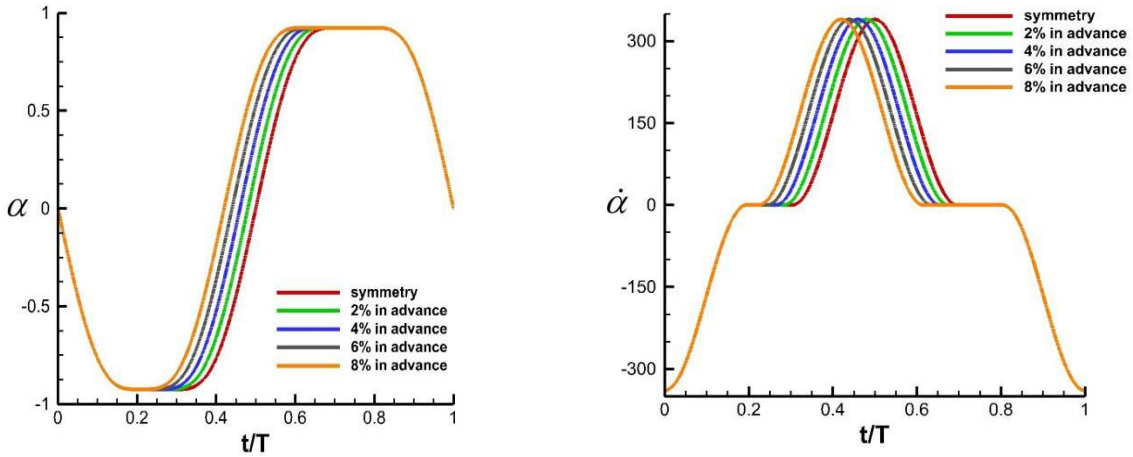

(a) attack angle (b) attack angle velocity

Figure 7. Angle of attack and angular velocity rates of four advanced rotations

3.1 Results of advanced models

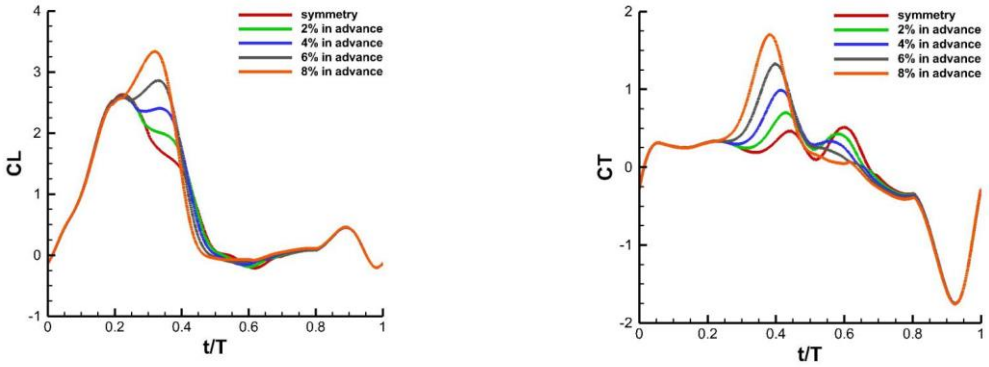

(a) the vertical force coefficients (b) the thrust force coefficients

Figure 8. Time courses of CL and CT for four advanced models

Figure 8(a) shows the profiles of CL for the four advanced models while Figure 8(b) shows the profiles of CT. The significant change happens during the time t/T from 0.22 to 0.41. CL has a dramatically increasing when the earlier advanced action happens. The period-averaged CL even increases 9% for 8% advanced model compared with no advanced mode. CT also increases during those time range which means resistance becomes larger in order to complete the advanced motion.

3.2 Energy consumption

Table 2. Time-averaged aerodynamic parameters for four advanced models

model	$\overline{CL}$	$\overline{CT}$	$\overline{CP}$	M
Symmetry	0.7374	-0.0593	0.196	1.328
2%	0.7642	-0.0368	0.214	1.242
4%	0.7946	-0.0124	0.242	1.128
6%	0.8240	0.0134	0.275	1.015
8%	0.8522	0.0401	0.312	0.916

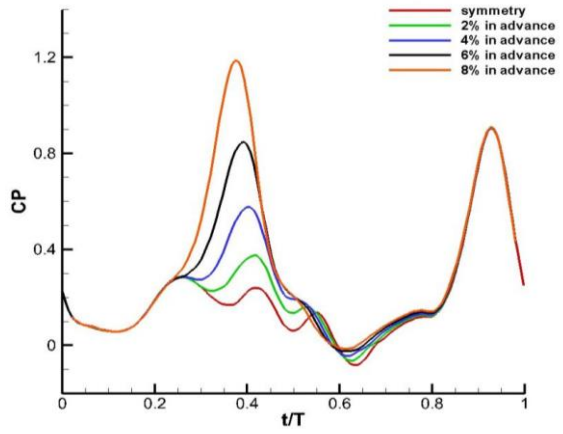

Figure 9. The profile of power coefficients Cps for four advanced models.

The aerodynamic parameters, including period-averaged CL, CT, power coefficient, CP, as well as figure of merit, M are calculated and summarized in table 2. And Figure 9 shows energy consumption of wing at one flapping period, which is calculated by the following formulation:

$$CP = \int_0^1 \oint_A (\vec{U}(t) \cdot \vec{n}(t))\, p(t) dA(t) d(t) \tag{5}$$

Moreover, the figure-of-merit M, is calculated by using the theory of Granlund, Ol, and Bernal [8] which is:

$$M = \frac{\overline{Cl}^{2/3}}{2P(2A_0 / c)^{1/2}} \tag{6}$$

Table 2 shows the time average CP increases with increasing the advanced time. The maximum value reaches to 0.3118 for 8% that means although the advanced model could improve lift force, the increasing of energy consumption has to be suffered.

4. Conclusion

In the paper, a novel numerical method is present to numerically investigate life force generation mechanisms of 3D dragonfly wing during hovering motions. A high lift force generated by implementing one specified advanced flapping action during hovering motion in which the translation time period of downstroke is shorten. The aerodynamic performance of different advanced models are numerically investigated compared with the values of the traditional symmetric model. The period-averaged CL increases 9% for 8% advanced model compared with no advanced mode. Although the advanced model could improve lift force, the increasing of energy consumption has to be suffered.

Acknowledgments

This research is supported by The National Natural Science Foundation, project No: 11672059. The financial support is gratefully acknowledged.

References

[1] Sane S P. The aerodynamics of insect flight[J]. J Exp Biol, 2003, 206(23):4191-208.
[2] Rozhdestvensky K V, Ryzhov V A. Aerohydrodynamics of flapping-wing propulsors[J]. Progress in Aerospace Sciences, 2003, 39(8):585-633.
[3] Lehmann F O. The mechanisms of lift enhancement in insect flight[J]. Die Naturwissenschaften, 2004, 91(3):101-22.
[4] Wang Z J. Dissecting insect flight[J]. Annual Review of Fluid Mechanics, 2005, 37(1):183-210.
[5] Sun M, Lan S L. A computational study of the aerodynamic forces and power requirements of dragonfly (Aeschna juncea) hovering[J]. J Exp Biol, 2004, 207:1887-1901.
[6] Norberg, R. A. The pterostigma of insect wings and inertial regulator of wing pitch[J]. Journal of Comparative Physiology, 1972, 81, 9-22.
[7] Norberg, R. A. Hovering flight of the dragonfly Aeschna juncea L., kinematics and aerodynamics[J]. In Swimming and Flying in Nature. 1975, pp. 763-781.
[8] Granlund, K., Ol, M., and Bernal, L. Quasi-Steady Response of Free-to-Pivot Flat Plates in Hover," Journal of Fluids and Structures, Vol. 40,July 2013, pp. 337–355.